ABIOMED WORKSHOP ON ULTRASOUND IN BIOMEASUREMENTS, DIAGNOSTICS AND THERAPY,
(PP. 153-172), GDANSK, 7TH – 9TH SEPTEMBER 2004

TRANSIENT ELASTOGRAPHY AND SUPERSONIC SHEAR IMAGING

M. FINK and M. TANTER

Laboratoire Ondes et Acoustique, ESPCI, Université Paris 7,
UMR CNRS 7587, 10 rue Vauquelin, 75005 Paris, France

Ultrafast ultrasonic imaging seems to have a strong potential for medical imaging applications. During the past five years, it has been applied successfully to quantitative assessment of soft tissues elasticity. An ultrafast ultrasonic scanner was built in our lab for quantitatively mapping the shear elasticity of soft tissues. The ultrafast Scanner provides images of the echogenecity of tissues similar to a standard echographic device but with a 200 times higher a frame rate. It allows to detect fast tissue motion induced by low frequency shear waves inside the body. From these displacements, a shear elasticity map is constructed using inverse problem algorithms. Preliminary in vivo results in breast demonstrate that this technique, known as transient elastography, is very sensitive to the presence of hard tumors. The same technique can also be combined with remote palpation induced par ultrasonic radiation pressure replacing the usual external vibrating system The same probe allows both to generate and detect shear waves propagation by using an unusual emission-reception sequence.

I. INTRODUCTION

By inducing motion in soft tissues, Elastography became a wide medical application field to study soft tissue mechanical properties. The technique developed by our group [1][2][3], called Transient Elastography, consists in generating a pulsed low frequency excitation at the surface of the tissue. The shear wave generated has a local propagation speed (typically 1 to 10 m/s) linked to the local Young's modulus. To be able to follow the transient shear wave propagation with ultrasound scanners, a very high frame rate (a few kHz) is needed. This is done by using an ultrafast imaging system which reduces the emitting mode to a single plane wave insonification. Frame rate up to 6000 images/s can be obtained. Solving the inverse problem of the shear wave propagation allows then to deduce the Young modulus image of the medium [4]. Compared to Static Elastography [5] or Sonoelasticity [6],

this ultrafast imaging technique has the advantage to be insensitive to patient motion and boundaries conditions artifacts and is not limited by shear wave reverberations. Recently, the beamforming process implemented on this ultrafast scanner was modified to achieve ultrafast estimation of both longitudinal and transverse displacements [7]. The displacements estimates were found to be improved by introducing an ultrafast compounded plane waves illumination process.
This paper presents a review of the basic principles of ultrafast imaging applied to transient elastography. In section II, the basic principles of ultrafast ultrasonic imaging are presented. In section III, the shear low frequency vibration induced for transient elastography is explained. In section IV, the data acquisition sequence and the local inversion processing allowing to recover the shear elasticity map of soft tissues are explained. Finally, in section V, the results of preliminary in vivo breast measurements on 15 women presenting a palpable tumor are discussed.

II. ULTRAFAST ULTRASONIC IMAGING SYSTEM

Since LF shear waves propagate at a few meters per second in soft tissues, thousands of frames per second must be acquired to follow their evolution on a centimeter scale with millimetric resolution. Standard ultrasonic scanners are limited to about 100 frames per second because these systems sequentially scan the medium. This sequential beam forming that results in the image formation is time consuming. A few high frame rate systems have been described. Shattuck et al [8] proposed to use a technique termed explososcan that increases by a factor of four the data acquisition rate of phased array scanner. Lu [9] used a Fourier method for high frame rate 2D and 3D pulse-echo imaging. Our approach is based on the delay and sum method associated to a single focalization in the receive mode. We developed an ultrafast ultrasonic imaging system based on a time reversal mirror electronic apparatus.

a. Principle

Ultra-fast imaging is obtained by avoiding focusing in transmit mode. A single emission is used to illuminate the whole medium. It consists of a quasi plane wave (Fig. 1(a)). Each element of the array features its own memory that is used to store the back-scattered (BS) signals or RF signals (Fig. 1(b)). As soon as reception is completed, the transducer can be used to emit a new signal and store other BS signals. The number of frames that can be stored depends on the amount of available memory. Without any focusing in transmit mode, the frame rate is only limited by the ultrasound travel time. In a 7.5 cm deep tissue-equivalent medium the ultrasound travel time is 100 μs which physically limits the frame rate to 10,000 frames per second. Parallel beam forming (PBF) is carried out afterwards numerically.

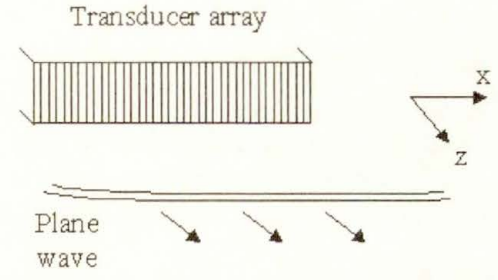

(a)

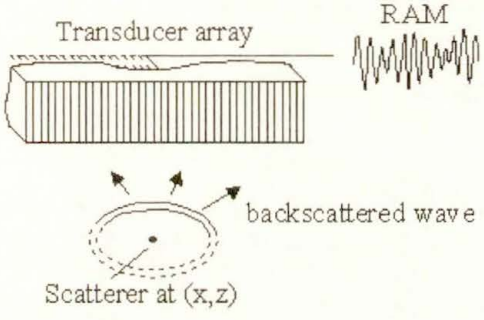

(b)

Fig. 1. The ultrafast imaging sequence. (a) The medium is illuminated using a plane wave. (b) Backscattered signals are stored in channel memories.

b. Parallel Beamforming

Parallel Beamforming (PBF) is performed in a second step using the delay and sum method. The pitch of the linear transducer array is *d*. The position in the image area is referenced as (x,z) (Fig. 1(b)). The plane wave reaches this position at time *z/c* after emission (c is the speed of sound). If a scatterer is present at this position, the plane wave is backscattered. The distance traveled by the BS spherical wave before reaching the i*th* element is

$$d_i(x,z)=\sqrt{z^2+(x-id)^2}\ . \tag{1}$$

Thus, the time needed for the plane wave to reach the scatterer at position (x,z), be backscattered and get to the i*th* element is

$$t(i,x,z)=\frac{z+\sqrt{z^2+(x-id)^2}}{c}. \tag{2}$$

Finally the beam formed RF signals $r_{BF}(x,t)$ are expressed as

$$r_{BF}(x,t=2z/c)=\sum_{i=0}^{N-1}\alpha(i,x,z).r_i(t(i,x,z)) \qquad (3)$$

where $r_i(t)$ is the ultrasonic signal received by the *ith* element and $\alpha(i,x,z)$ is an apodization factor. Instead of a dynamic focusing in receive mode which is time consuming since calculations are performed by the computer, we use several focal zones as in some modern scanners. The time delay law $t(i,x,z)$ is discretized over depth. The k*th* focal distance is f_k. A single time delay law is used in each focal zone. The focal zone length, l_k, is chosen in order not to exceed the theoretical full length at half maximum which depends on the wavelength, aperture and focal distance

$$l_k < 7\lambda\left(\frac{f_k}{D}\right)^2 \qquad (4)$$

where D is the aperture and λ the wavelength.

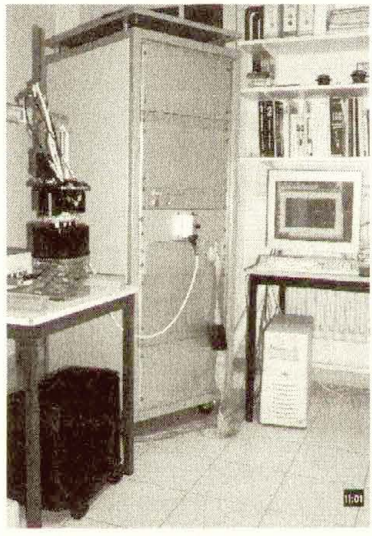

Fig. 2. The fully programmable electronic system.

c. Electronics

The fully programmable electronic system (Fig. 2) used to emit and receive ultrasonic signal features 128 independent channels with 2 Mbytes random access memory (RAM) each and a sampling frequency of 50 MHz. A numerical summator is used to perform the delay and sum algorithm. The center frequency of the linear array of 128 transducers is 4.3 MHz and its bandwidth is about 70 %. The system can be used to produce ultrasonic images. Two acquisition modes are implemented. The first mode corresponds to the standard ultrasonic scanner image formation with focalizations in transmit and receive modes. It reaches frame rates of about

50 frames per second. The second mode is used to produce up to 10,000 frames per second using a single focalization in the receive mode.

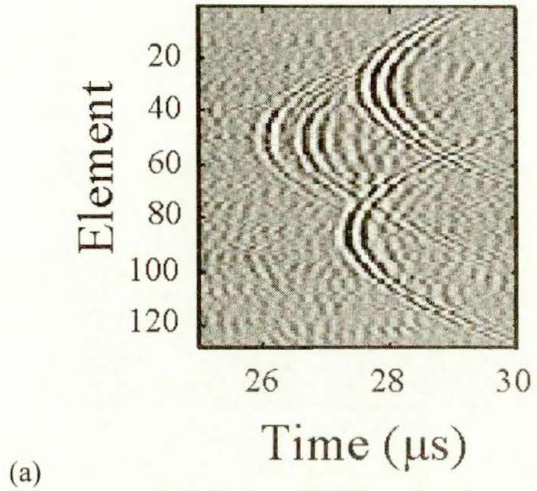

(a)

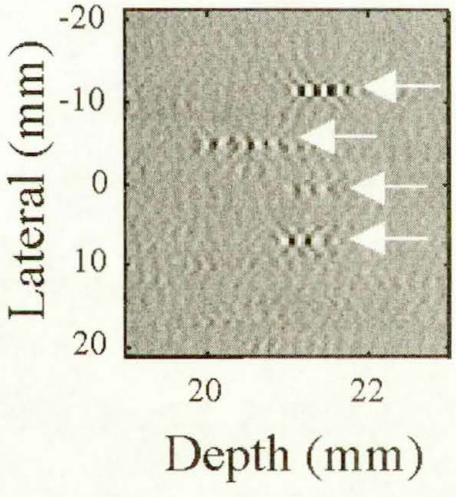

(b)

Fig. 3. Tissue-equivalent phantom containing line targets. (a) RF responses received by the 128 elements of the transducer array. (b) RF image obtained after PBF. The line targets are indicated with white arrows.

The ultrasonic data are stored into the channel RAM and the ultrasonic images can be computed afterwards numerically. Since the duration of the response that must be stored on each channel in order to construct an ultrasonic image is typically about 100 μs (5000 points), the maximum number of frames that can be stored in the 2 Mbytes RAM is about 400.

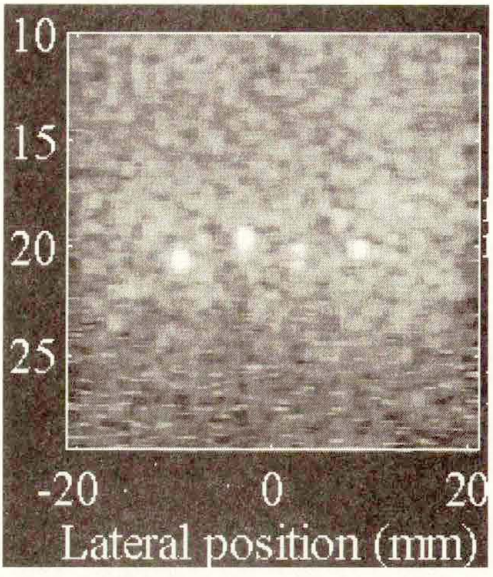

(a)

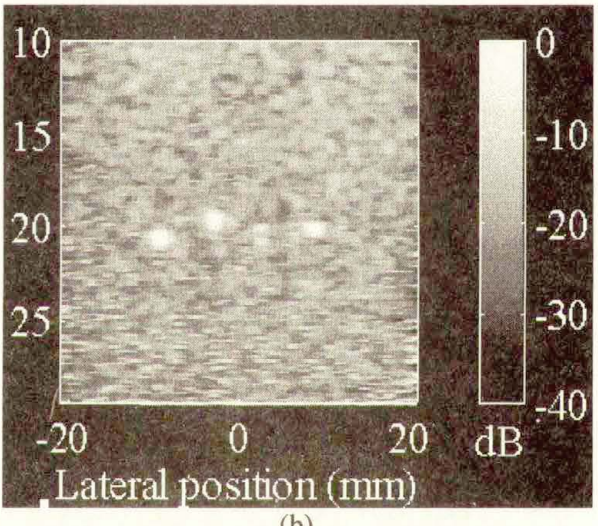

(b)

Fig. 4. Ultrasonic images (after demodulation) obtained in the tissue equivalent phantom containing line targets. Comparison between (a) the standard transmit-receive focalization mode and (b) the ultrafast imaging single focalization mode.

d. Applications

Fig. 3(a) shows a 5 μs duration window of the 128 elements RF responses obtained during an experiment on a tissue-equivalent phantom containing line targets. The echoes of the line targets superimpose with the ultrasonic speckle pattern coming from the randomly distributed scatterers. The Fig. 3(b) presents the corresponding 42×4 mm^2 region of the computed RF image using the single focalization in receive mode. This image is termed RF image since it is not demodulated. The targets are clearly localized (white arrows).

The consequences of a plane illumination have been investigated using the ultrafast ultrasonic imaging system that can also be used to produce standard ultrasonic images with double focalization in transmit and receive modes. Comparison between both imaging modes is presented in Fig. 4 for demodulated ultrasonic images. The first consequence is a degradation of the lateral resolution. The second consequence is a decrease of image dynamic and signal to noise ratio. However high dynamic range is not needed in our experiments since we only intend to perform cross-correlation between consecutive RF images. The reduced image quality should not affect the displacements estimation.

III. SHEAR WAVE GENERATION

In soft tissues the shear modulus is less than 1 MPa while the compression modulus is of the order of 1 GPa [10]. Thus, at a fixed strain, shear displacements would be much larger than compression displacements if shear and compression attenuations were identical. But the frequency dependence of shear attenuation and compression attenuation differs. Shear waves are fully attenuated at ultrasonic frequencies. This explains why soft tissues behave like water for ultrasound. On the contrary, at low frequencies (less than 200 Hz), shear attenuation is low and shear waves may be induced using an adapted low-frequency vibrating device.

In our first experiments, shear waves were generated using a LF vibrating device composed of two parallel rods. The distance between the two rods is equal to 3 cm. The LF signal generally consists in one period of a sinusoid (typically 50 Hz). As shown in Fig. 5. , the linear array of transducers is placed between the rods that are fixed to two electromagnetic vibrators (Bruel & Kjaer minishaker n°4810). The rods are parallel to the active surface of the array. The dimension of the part of the rod that is in contact with the medium is 80 mm × 4 mm. The set of rods and the transducer array are independent, so the transducer array remain fixed while the rods are vibrating.

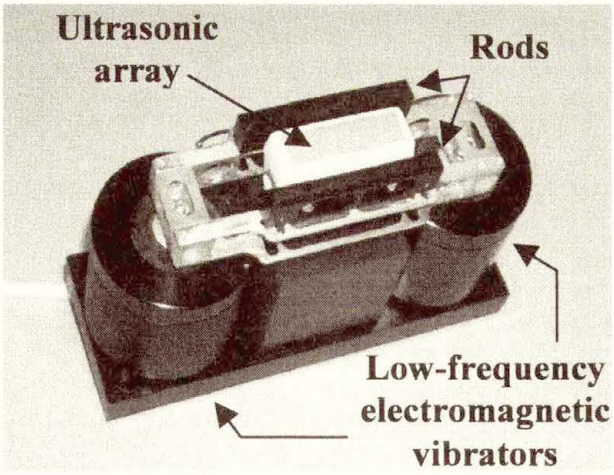

Fig. 5. The LF vibrating device.

However, this first system was not optimally convenient for in vivo breast measurements. Physicians preferred to use a more compact system and we finally decided to generate the transient push at the surface of the breast with the front side of the transducer array itself. Thus, the ultrasonic probe was mounted on the vibrating system as presented on Fig. 6.

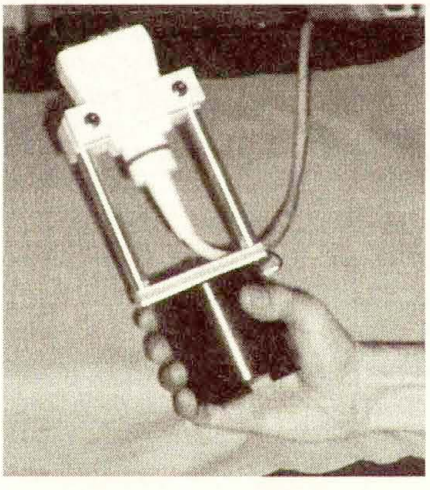

Fig. 6. Improvement of the mechanical system for preliminary clinical investigations in breast cancer detection : Ultrasonic probe mounted on the low frequency *vibrating* device

IV. DATA ACQUISITION AND INVERSION ALGORITHM

a. Data Acquisition

The RF signals are acquired at a high frame rate (typically 1,000 frames per second) during the propagation of the LF shear waves (Fig. 7). The RF and displacements images are computed afterwards numerically. Many speckle tracking algorithms [11] have been developed in order to estimate the axial or even lateral displacement or strain [12] in soft tissues. In our study speckle lines are segmented versus depth z into about 2 mm slices with 50 % overlap. The axial displacement is estimated in each of the segments using a cross-correlation technique between consecutive RF images. The precision on axial displacement is about 1 μm.

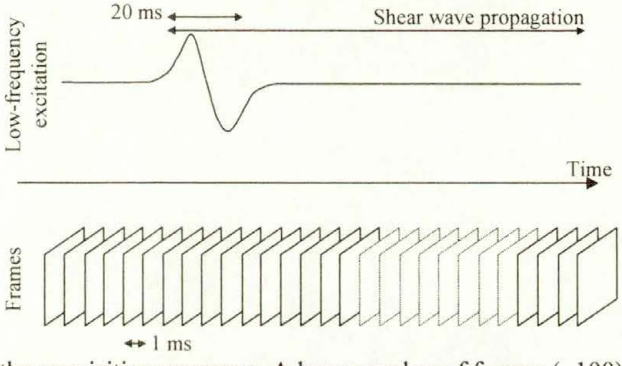

Fig. 7. Details of the acquisition sequence. A large number of frames (~100) are acquired at a high frame rate (every 1 ms) while the LF shear wave (~50 Hz) propagates through the medium.

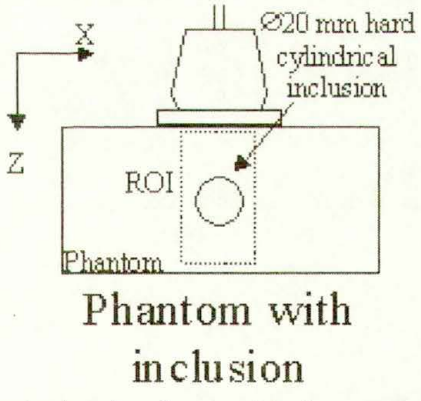

Fig. 8. The vibrating device is placed on the top of the heterogeneous phantom.

As shown in Fig. 8, the ultrasonic probe was placed on the top of the phantoms. The ultrasonic array vibrates vertically. The excitation central frequency is 50 Hz and the amplitude of the axial displacement is about 1 mm. The excitation lasts one period (20 ms). 100 frames are acquired at a rate of 1000 frames per second. Thus the

acquisition time reaches 100 ms. The axial (in the z-direction) displacement images induced in the heterogeneous phantoms by the propagation of the 50 Hz shear wave are presented in Fig. 9 for different times. The maximum amplitude of the axial displacement at 50 mm depth is about 100 μm but it is much higher close to the array. The presence of the heterogeneity largely affects the propagation of the shear wave. The shear wave front remains quasi linear (Fig. 9 (b)) until it reaches the hard inclusion in which the shear velocity is larger. The shear wave propagates faster in the inclusion with smaller axial displacements due to the larger Young's modulus. In the inclusion, the shear wave front bends and the axial displacements amplitude decreases (Fig. 9 (d)).

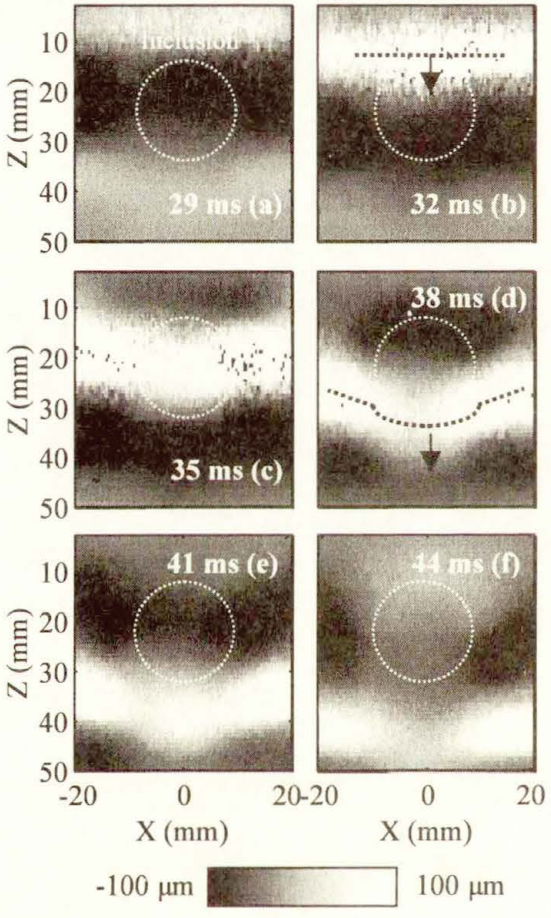

Fig. 9. Heterogeneous phantom with an inclusion. Evolution of the axial displacement during the shear wave propagation from the top to the bottom. The shear wave front and the inclusion contour are respectively indicated.

b. Inversion processing

The need for quantitative information yielded to the development of an inversion algorithm. It consists in reconstructing the shear modulus distribution map using a direct and local inversion of the spatio-temporal data. As explained in detail in ref [2], this local inversion is achieved by calculating the ratio between spatial and temporal derivatives of the longitudinal displacements $u_z(x,z,t)$
By making the assumption

$$\frac{\partial^2 u_z}{\partial y^2} << \frac{\partial^2 u_z}{\partial x^2} + \frac{\partial^2 u_z}{\partial z^2} \tag{5}$$

that is only valid if there is no out of plane gradient for the shear field, it is easy to estimate locally the shear modulus in the elastic medium:

$$\mu(x,z) = \rho \frac{1}{N} \sum_{n=1}^{N} \frac{\left(\frac{\partial^2 u_z}{\partial t^2} \right)_{x,z}}{\left(\frac{\partial^2 u_z}{\partial x^2} + \frac{\partial^2 u_z}{\partial z^2} \right)_{t=nT}} \tag{6}$$

where T is the period of frame acquisition and N is the number of displacement images. This algorithm allows to recover the shear modulus spatial distribution corresponding to displacement movie presented in Fig. 9. It is presented in Fig. 10. The hard inclusion is clearly recovered.

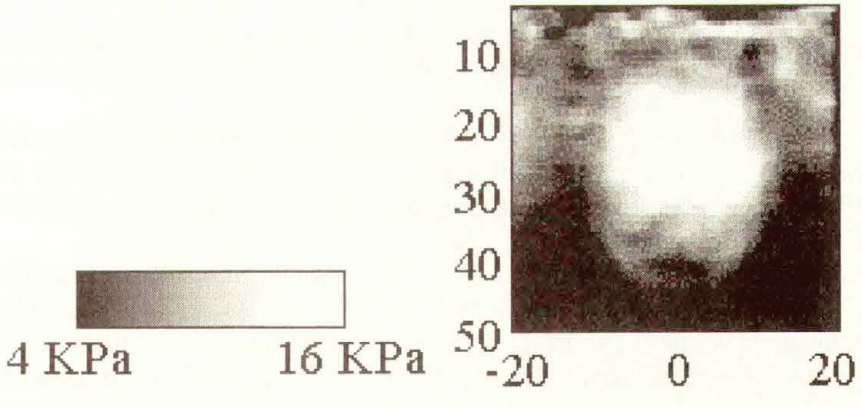

Fig. 10. Shear modulus distribution map in the phantom with an inclusion. The layers and inclusion are clearly localized.

This algorithm allowed us to image very properly local hard inclusions of 5 mm diameter. The interesting point is that the optimal resolution of this imaging system is not limited by the wavelength of the shear wave (of the order of a centimeter) but by the resolution of the ultrafast scanner. The reason for this is that the displacement field is measured at every point **inside** the medium and so the high resolution of the shear elasticity maps achieved experimentally is around 2 mm. The inverse problem solving can rely on a hyper-resolution property.

c. Validity of equation (5)

A numerical simulation based on Green's function formalism was used to calculate the shear displacements induced in an homogeneous elastic medium by both vibrator systems. The goal is here to estimate and compare the diffraction effects induced by the two vibrating devices (2 rods or probe) and check the validity of the assumption described by equation (5) during the inversion process.
A low frequency propagating shear wave is simulated in a soft isotropic and homogeneous media. The code is based on Lhemery's (1994) Green's function for a semi-infinite media associated to a source points set. The two different kind of sources tested are shown in Figure 5. In order to mimic soft tissues properties a medium with the following characteristics has been simulated: a compression velocity of 1500 m/s, a shear velocity of 2 m/s and density of 1000 Kg/m^3. The Green function is estimated in a 40×40 mm zone sampled with a 0.5 mm step. This area correspond to the $(x,z)_{y=0}$ plan and is represented by the dash line on Figure 11

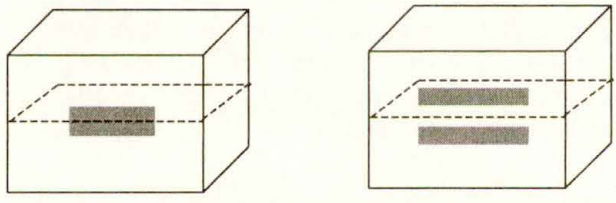

Fig. 11. (a) a rectangular 15×55 mm source (identical to the probe). (b) two parallel rectangular 10×80 mm sources. The plane presented by the dash line is the corresponding experimental imaging zone.

The displacements u_z induced in the medium were obtained by convolving the simulated Green's function by a pulse with a 60 Hz central frequency. We note that the displacements induced by the two rods (b) are bigger than the ones created by the array itself (a).
The inverse problem is then applied to these two simulated displacements. The shear velocity maps are shown in the Figure 6. In both cases, the shear velocity is overestimated in the very near field where equation (5) is no more a valid assumption. Nevertheless, the shear speed estimation is valid in a large area of the image.

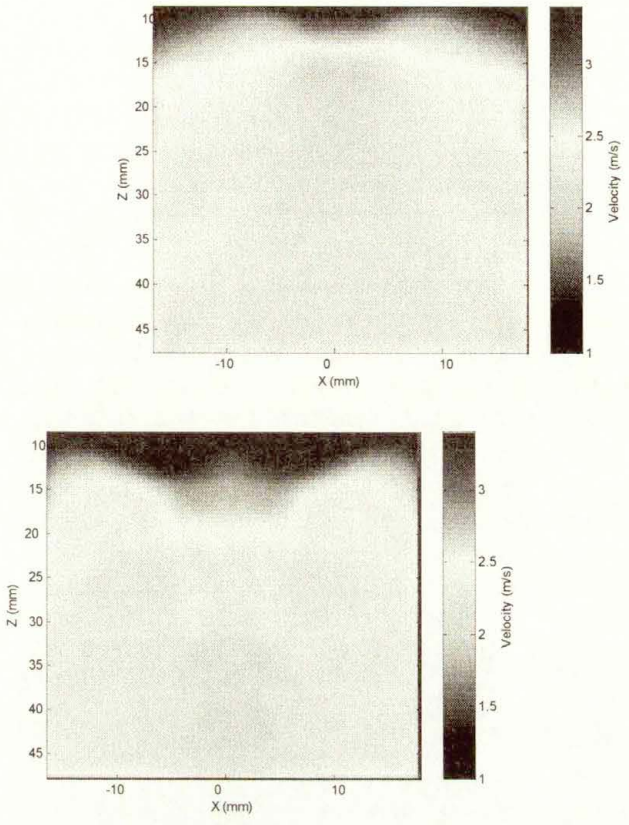

Fig.12. Reconstruction of the velocity map for (top) a rectangular source (below) two parallel rectangular sources.

Simulation shows that, regarding to the diffraction effects, the elasticity estimation using the new vibrator is better in the near field than the one with the two rods. The use of the array as a vibrator appears to be an interesting solution as it gives clean reconstruction maps while being easier to use than the old vibrator device.

V. IN VIVO CLINICAL RESULTS ON BREAST

In this section, the preliminary results of the *in vivo* validation of the transient Elastography are reported. The aim of this study was to demonstrate that nodules can be detected using our elastography technique. For this first validation, patients whose tumors were palpable (usually more than 15 mm diameter) and visible on echographic scans has been chosen. This study was realized at the Curie Institute, with the collaboration of the radiology departement.

a. Patients and study protocol

A total of 15 patients with mean age of 61±16 years and age ranging between 31 and 90 years were included in this study. All subjects had a palpable breast lesion and had to undergo a biopsy and a surgical operation after the elastography evaluation. All the patients gave their consent to be examined by our elastographic device. The histologic results shows that only one patient has a benign lesion and all the others had an adenocarcinoma lesion. The measurements were made with the collaboration of a radiologist. Each patient was lying, chest naked, on a bed (Fig. 13). First the doctor localized the nodule by palpation, then he positioned the array system and localized the tumor using a conventional echographic image provided by our ultrafast imaging system and finally, when the imaging plane is correct he realized the elastographic acquisitions (ie the transient vibration and tha ultrafast acquisition). The echographic image and the elasticity measurement are performed using the same machine. The low frequency impulse (a 60Hz frequency centre pulse) excited the breast of the patient while the ultrafast scanner records 250 frames at a 3000 Hz repetition rate. The total duration of the examination of one patient is about 10 minutes, and 3 successive measurements were carried out. The acquisition is instantaneous (0.075 seconds) but saving data needs about 2 minutes.

(a)

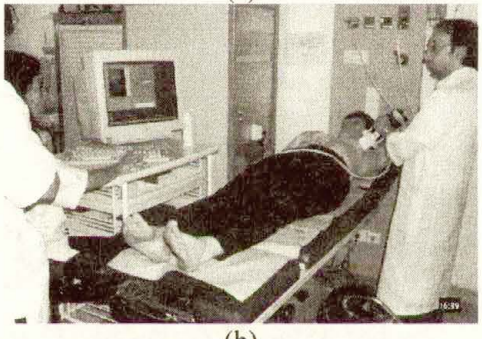

(b)

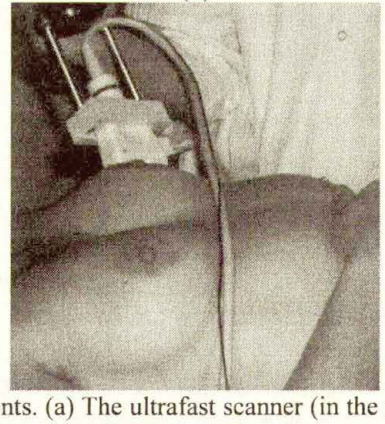

Figure 13: *In Vivo* experiments. (a) The ultrafast scanner (in the middle of the picture) works as a standard echographic device while the physician (on the right) locates a potential region of interest. (b) A low frequency impulse is then sent while 250 frames at a 3000 Hz repetition rate is recorded to memory.

b. Results

For each patient two images were performed: an echographic and an elasticity image. Most patients (eleven of them) presented tumors visible on the echographic images. The four patients whose tumor did not appear on the echographic image were eliminated from this study. Most lesions were superficial and only two patients had a cancerous tumor deep in the breast. The inversion algorithm described above was applied to the displacement movies of the *in vivo* measurements. Thus, an elasticity map was performed for each patient.

Fig. 14 shows one example of shear modulus images obtained on a 46 years old volunteer and their corresponding echographic images (Fig. 14-a, Fig. 14-b). The nodule located on the right breast were superficial, palpable and perfectly visible with echography. In the echographic images the upper zone represents the reflectivity of the breast, the dotted curve represents the ribs.

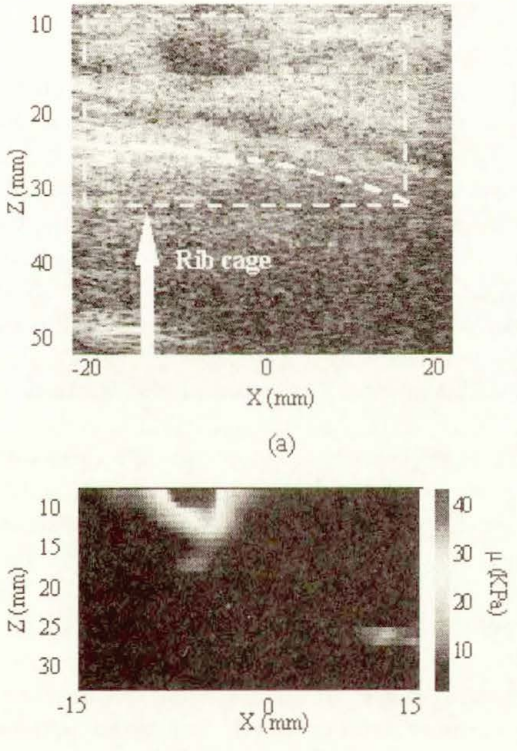

Figure 14 : Comparison between the ultrasonic image (**a**) and the corresponding shear elasticity map (**b**) of breast for one patient. A hard tumor (adenocarcinoma) appears as a dark area on the ultrasonic image and as red or yellow on the shear elasticity map. The elasticity maps correspond to the dashed rectangle on the ultrasonic images.

A biopsy indicates that the dark area on the top is an adenocarcinoma. The inverse problem is applied in the area inside the dashed line and gives the shear elasticity maps. The tumors are also visible on the elasticity images. The adenocarcinoma, which is the red or yellow region of the upper part appears to be 5 harder than the surrounding healthy tissue respectively. Its localization is not atypical and one remarks that transient elastography is able to detect and characterize tumors at the surface of the breast.

Among the 11 patients examined using our transient system, 6 of them (55 %) presented a hard lesion on the elasticity map. The existence and the location of these tumors were confirmed by the ultrasonic images. All of these 6 patients have a superficial and palpable tumors of a few centimeter diameter. Biopsy demonstrated that they all have an adenocarcinoma lesion.

c. Discussion

This first *in vivo* clinical protocol was realized in collaboration with the Curie Institute. The goal was to validate, *in vivo*, the transient elastography technique by detecting cancerous nodules on the elasticity images. Among the 15 examined patients 6 of them presented a clear visible tumor both on the ultrasonic and the elasticity image. These preliminary results are very encouraging because we were able to show the first *in vivo* elasticity images of women's breast cancer achieved by the transient elastography technique. In fact, the protocol was established to examine patients with a palpable tumor in an advanced stage of the disease. Thus tumors were visible on ultrasonic images. Why didn't we detect tumors on the elasticity map of all the patients chosen for this study? Several reasons can be evoked. First the ultrasonic mode was achieved with the our ultrasonic device (which doesn't contain a hardware beamforming system) to simplify the tumors localization by the radiologist, the frame rate of this mode was about 2 images per second which is not very efficient compared to the 50 images per second of a classical ultrasonic scanner. This could have caused a time shift between the tumor visualization on the screen and the elastographic acquisition during which the tumor was no more in the imaging area. For this reason, four patients were even removed from this study because they did not present visible tumors with the ultrasonic exam. The other reason can be related to the excitation source. In fact, if the array surface is not properly in contact with the patient's breast, the shear wave generated will propagate differently and will probably cross the imaging plane instead of propagating in the imaging plane. In that case, the out of plane spatial variations of displacements can no more be neglected. For these patients, the displacement movies show more a wave beating than a wave front propagation. In other words, when there is an out of plane motion, the assumption $\frac{\partial^2 u_z}{\partial y^2} << \frac{\partial^2 u_z}{\partial x^2} + \frac{\partial^2 u_z}{\partial z^2}$ is not valid and a good reconstruction of the inverse problem is not possible any more.

Up to date, our efforts have been focused on the localization of the cancerous tumors. The reconstructed images show perfectly the contrast between healthy and cancerous tissues. The shear elasticity map is computed from the z-component of the

displacement normal to the array (u_z). Recently, we have learned how to determine the x-component of displacements (the transverse displacement that is perpendicular to the array axis) [7]. This additional information should improve the final shear elasticity mapping.
Compared to methods using static deformations [5] the advantage of systems based on transient shear wave propagation is that no prior knowledge of the boundary conditions is needed to quantitatively estimate the young modulus or the shear elasticity. Moreover, a 80 ms experiment is sufficient in transient elastography. It corresponds to the time needed for the shear wave pulse to cross the whole medium. Consequently, compared to Doppler ultrasound based techniques [6] or magnetic resonance methods using a monochromatic shear wave, transient elastography avoids the reconstruction difficulties that arise first from nodes of vibrations and second from disturbing motion within the long experiment times (e.g.,breathing, heartbeat).

V. REMOTE PALPATION AND ULTRAFAST IMAGING

Recently, we have extended the Transient Elastography technique by using a new way to generate pulsed shear wave excitation [13] : the use of the acoustic radiation force by focusing an ultrasound beam at a chosen location during a long application time (typically 50 to 100 microseconds). It creates a remotely transient shear wave source inside the medium The advantage of this technique lies in the number of shear sources and locations that can be arbitrarily and adaptively chosen according to the experience and the medium characteristics. After its generation, the shear wave propagation is imaged by the ultrafast scanner. Results demonstrate that a unique ultrasonic array can be used for both the generation of a single transient shear wave and the ultrafast imaging of the its propagation across the whole image plane. Our fully programmable electronics allow to induce and image, as desired, several shear sources at different times and locations in order to compute a real "shear wave beamforming" and optimize the shear source shape to the studied medium. For example we show that by using a moving shear source that move in the tissue at supersonic celerity we can generated quasi plane shear waves that make any angle of incidence in the tissue. From the movie of this shear waves propagating in the medium (Fig. 15.), an elasticity image of the whole medium can be recovered using only a few pushing beams (1 to 5) see Fig.. 16.

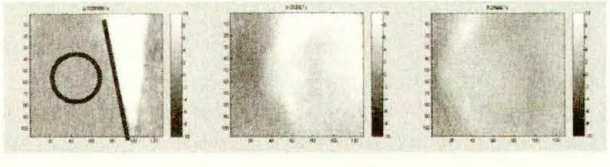

Figure 15: Shear plane wave propagating through a harder inclusion

A plane wave front is induced by radiation force and it is clearly distorted and accelerated when it propagates through the inclusion. The data is then used to reconstruct the shear velocity map of the medium:

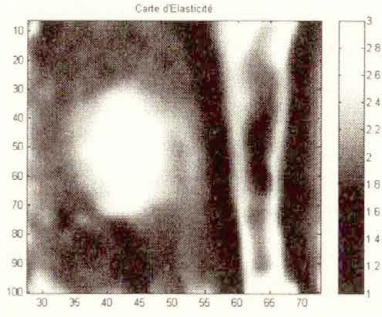

Figure 16 : Shear velocity reconstruction of the heterogeneous medium

VI. CONCLUSION AND PERSPECTIVES

Transient elastography based on the use of an ultrafast ultrasonic scanner has been successfully applied to quantitative imaging of soft tissues elasticity. First clinical results for breast elasticity imaging are very promising. In the near future, three poles of interest are to be studied. First, the off-line computation of the beam forming process should be replaced by hardware to permit real-time conventional echographic imaging and should lead to an easier positioning of the array by the physician regarding to the region of interest. Secondly, because there is no fundamental limit which prevents the use of transient elastography with 2D ultrasonic arrays, a generalization of the current algorithm should lead to a 3D shear elasticity mapping. Finally, the coupling of ultrafast scanner with internal vibration induced by the acoustic radiation force is very promising and recent experiments show that it should be possible to remotely induce a shear wave and image its propagation with a single ultrasonic array.

We speculate that transient elastography may have a preponderant role as an ultrasonic quantitative palpation technique to detect tumors of breast, liver or kidney in the next decade.

REFERENCES

[1] S. Catheline, J-L. Thomas, F. Wu, M. Fink.« Diffraction Field of a low frequency vibrator in soft tissues using transient elastography ». ". IEEE Ultr. Ferr. And Freq. Ctrl 46, (4), July 1999, p.1013-1019.

[2] L. Sandrin, M. Tanter, S. Catheline, M. Fink. "Shear Modulus Imaging with time resolved 2D pulsed elastography". IEEE Ultr. Ferr. And Freq. Ctrl. 49 (4), April 2002 p 426-435.

[3] L. Sandrin, M. Tanter, S. Catheline, M. Fink " Shear elasticity probe for soft tissues with time resolved 1D pulsed elastography" IEEE Ultr. Ferr. And Freq. Ctrl. 49 (4), April 2002, p 436-446

[4] T.E. Oliphant, R.R. Kinnick, A. Manduca, R.L.Ehman, J.F.Greenleaf, "An error analysis of Helmholtz inversion for incompressible shear vibration elastography with application to filter design for tissue characterization,"in Proc. IEEE Ultrason. Symp.,2000,pp.1795 –1798.

[5] J. Ophir, E. I. Cespedes, H. Ponnekanti, Y. Yazdi, and X. Li. "Elastography : A method for imaging the elasticity in biological tissues", Ultrason. Imaging, 13, pp 111-134, 1991.

[6] R.M.Lerner, K.J.Parker, J.Holen, R.Gramiak, R.C Waag, "Sono-elasticity: Medical elasticity images derived from ultrasound signals in mechanically vibrated targets,"Acoust. Imaging ,vol.16,p.317 –327,1987.

[7] M. Tanter, J. Bercoff, L. Sandrin, M. Fink,"Ultrafast compound imaging for 2D motion vector estimation : Application to transient elastography" IEEE Trans. Ultrason., Ferroelec. Freq. Contr. 49 (10), 2002,p 1363-1374

[8] D.P Shattuck,. M.D Weinshenker, , S.W Smith. and O.T Von Ramm, "Explososcan: A parallel processing technique for high speed ultrasound imaging with linear phased arrays", J. Acoust. Soc. Am. 75 (4), pp. 1273-1282, 1984.

[9] J. Lu, « 2D and 3D High Frame Rate Imaging with Limited Diffraction Beams », IEEE Trans. Ultrason. Ferroelectr. Freq. Contr., vol. 44, N°4, 1997.

[10] A.Sarvazyan, "Biophysical bases of elasticity imaging", Acoustical Imaging, 21, Plenum Press, New-York, pp. 223-240, 1995.

[11] M., O'Donnell, A.R Skovoroda,., B.M Shapo, Y, Emelianov,., "Internal Displacement and Strain Imaging Using Ultrasonic Speckle Tracking", IEEE Trans. Ultrason. Ferroelectr. Freq. Contr., vol. 41, N°3, pp. 314, 1994.

[12] E. Konofagou, J.Ophir, "A new elastographic method for estimation and imaging of lateral displacements, lateral strains, corrected axial strains and Poisson's ratios in tissues", Ultrasound in Med. & Biol., vol. 24, No 8, pp. 1183-1199, 1998.

[13] J.Bercoff, M.Tanter, S.Chaffai and M.Fink . "Ultrafast imaging of beamformed shear waves induced by the acoustic radiation force. Application to transient elastography", In the same proceedings of IEEE Ultrasonics, Munich 2002